The Effect of Basic-State Potential Vorticity Gradients on the Growth of Baroclinic Waves and the Height of the Tropopause

NILI HARNIK AND RICHARD S. LINDZEN

Department of Earth, Atmospheric, and Planetary Sciences, Massachusetts Institute of Technology, Cambridge, Massachusetts

(Manuscript received 28 May 1996, in final form 27 May 1997)

ABSTRACT

The stability characteristics of normal mode perturbations on idealized basic states that have meridional potential vorticity (PV) gradients that are zero in the troposphere, very large at the tropopause, and order β in the stratosphere are checked. The results are compared to the corresponding models that have a lid at the tropopause. The dispersion relations and the vertical structures of the modes are similar in the two models, thus confirming the relevance of the Eady problem to unbounded atmospheres. The effect of replacing the lid with a more realistic tropopause is to complicate the interaction of tropopause and surface waves, such as to inhibit phase locking for a range of wavenumbers. This causes the short-wave cutoff of the Eady model to move to longer waves. Also, there is a slight destabilization of the long waves, which have large amplitudes in the stratosphere.

The effect of gradually changing the tropospheric PV gradients from zero (Eady-type profile) to β (Green-type profile) on the stability of normal modes is checked. The dispersion relations show a smooth transition from the Green profiles to the Eady profiles, and a short-wave cutoff is gradually formed.

Finally, the possibility of neutralizing the atmosphere through the short-wave cutoff of the Eady model by lifting the tropopause while keeping PV gradients zero in the troposphere is examined. It is found that instability depends on some minimal amount of tunneling of waves between the surface and the tropopause. The amount of tunneling depends on the vertical integral of N in the troposphere. It is necessary for $\int N\,dz$ to increase for the short-wave cutoff to move to longer waves. For reasonable Brunt–Väisälä frequency profiles, lifting the tropopause causes the short-wave cutoff to move to longer wavelengths, but the details are sensitive to boundary values of N^2 and wind shear.

1. Introduction

a. Motivation

What determines the zonal-mean flow of the atmosphere is one of the central problems of the general circulation. One of the theories that addresses this issue is baroclinic adjustment (Stone 1978). It is based on the notion that, on planetary scales, baroclinically unstable eddies will act to stabilize the mean flow from which they draw their energy, by analogy with convective adjustment. Since the forces responsible for the instability of the basic state are permanent, a balance will be set up between the eddies that are trying to drive the flow toward stability and the forcing that is trying to drive the flow away from it. The resulting basic state will be somewhere between the neutral state and the forced state (radiative equilibrium, in our case). How close this profile will be to neutrality depends on how the growth rates vary with the degree of instability and on the type and amount of dissipation in the system. All this depends on the existence of a realistically achievable neutral state. In existing theories, the neutralization mechanism is the tendency of the eddies to mix potential vorticity (PV) along isentropes (Rhines and Young 1982) and at the surface,[1] which will cause the meridional PV gradients in the system to decrease or be eliminated.

Previous studies (Stone 1978; Lindzen and Farrell 1980a; Cehelsky and Tung 1991; Stone and Branscome 1992; Gutowski 1985; Gutowski et al. 1989) focused on the neutral state, which results from wiping out the PV gradients in the lower part of the troposphere, including at the surface. In this way, the Charney–Stern criterion for stability (Charney and Stern 1962) is satisfied. This criterion states that a fluid will be stable only if the PV gradient does not change sign anywhere. In the atmosphere, a negative meridional temperature gradient at the surface is equivalent to a negative PV gradient there (Bretherton 1966). The planetary vorticity

Corresponding author address: Dr. Richard S. Lindzen, Dept. of Earth, Atmospheric, and Planetary Sciences, Massachusetts Institute of Technology, Rm. 54-1720, Cambridge, MA 02139.
E-mail: rlindzen@mit.edu

[1] Mixing PV at the surface means wiping out meridional temperature gradients there and/or increasing static stability to ∞.

gradient is positive; hence the natural tendency of the atmosphere is to have a positive PV gradient almost everywhere else. The only way to satisfy the Charney–Stern criterion is to wipe out the PV gradient in the lower part of the atmosphere and either to wipe out the temperature gradient at the surface (Lindzen and Farrell 1980a) or to increase the static stability to infinity at the surface (Gutowski 1985); neither of these is observed in the atmosphere on large scales.[2] This was demonstrated in a set of experiments performed by Gutowski et al. (1989), which consisted of running a nonlinear primitive equation model from an initially unstable state to steady state, with surface friction and surface heat fluxes and without them. The model with no forcing or dissipation adjusted to a neutral state by wiping out the PV gradients in the lower part of the troposphere as well as wiping out the surface temperature gradients and increasing N^2. The model with both surface fluxes and friction could not reach the same neutral state because it could not decrease the PV gradients at the surface to zero.

This raises the question of whether the eddies, faced with such a situation, have an alternative way in which they can neutralize the atmosphere. Lindzen (1993) suggested such a neutral state that is based on the short-wave cutoff of the Eady model. This cutoff is a direct result of the zero PV gradients in the interior of the model atmosphere. The zero PV gradient region does not allow internal Rossby wave propagation and, hence, limits the interaction between the two edge waves, one at the surface and one at the upper lid, which represents the tropopause. When the horizontal wavelength becomes short enough, the vertical decay of the edge waves is too fast for them to ''see'' each other and interact with the basic shear at the steering level. Hence, the location of the short-wave cutoff depends on the height of the lid. Moving the lid up would cause the short-wave cutoff to move to longer waves. If there is some meridional confinement that keeps the total wavenumber higher than some value (i.e., the width of the jet stream), complete neutrality could be achieved by moving the short-wave cutoff to that minimum wavenumber.

The reasoning behind all this is that unstable eddies will attempt to wipe out PV gradients as long as they exist, tending to bring the atmosphere to an Eady model state.[3] This can lead to eddies that are still unstable but have no more PV gradients to wipe out in the troposphere; it is plausible that they push the tropopause upward while concentrating the jet (thus increasing the meridional wavenumber), thus continuing to approach neutrality. Note that the tropopause is the edge of the mixing domain; it intersects the isentropic surfaces along which PV is mixed. The limiting neutral state differs from the Charney–Stern one in that it has zero PV gradients in the entire troposphere, not just at the lowest part of it,[4] and the meridional temperature gradient at the surface remains.

How close the atmosphere is to an Eady model is not a trivial question. There is some observational evidence that the eddies mix PV along isentropes (Morgan 1995; Sun and Lindzen 1994, Stone and Nemet 1996). The degree of mixing is hard to determine because PV is not measured directly; rather, it involves taking a second vertical derivative of directly observed quantities. The existing vertical resolution of observations is hardly fit for that. Sun and Lindzen (1994) and Lindzen (1994a,b) showed that the differences in the wind and temperature fields between a state of vanishing PV gradients and a state of PV gradients on the order of β are small, probably observationally indistinguishable. However, radiative equilibrium profiles have large enough PV gradients in the troposphere (a few β) for them to be observationally distinguishable from neutralized profiles. Stone and Nemet (1996) calculated the observed zonal-mean isentropic slopes[5] (which involve only first-order vertical derivatives) in the troposphere at different seasons and latitudes and compared them to the isentropic slopes of the radiative equilibrium state and the Charney–Stern neutral state. They found that in midlatitude winter, the middle troposphere (between 800–400 mb) is much closer to the neutral state than to radiative equilibrium, which suggests that the atmosphere is mixing PV to a significant extent. It is important to note here that, even if the neutralization theory works, the adjusted state of the atmosphere cannot be strictly neutral since enough instability must remain to balance dissipation and nonlinear processes.

Simple linear models of baroclinic instability are useful in studying what kind of neutral states exist in theory. These models may also give us a sense of how plausible it is for the atmosphere to reach them. The classical examples of such models are the Charney model (1947) and the Eady model (1949). The Charney model has been used to study the neutralization by the Charney–Stern criterion (Charney and Stern 1962), while the Eady model was naturally used by Lindzen (1993) to

[2] This mechanism of neutralization does seem to work on smaller scales. Homogenization of the temperature at the surface is often observed in storm tracks on synoptic scales, and has been demonstrated in modeling studies of baroclinic wave life cycles (Simmons and Hoskins 1978; Thorncroft et al. 1993 and references therein).

[3] An Eady model state refers to a state where there are no PV gradients in the troposphere. In the atmosphere, unlike in the Eady model, there is a meridional gradient of planetary vorticity (β); therefore, the wind and temperature have to vary with height in a certain way to cancel out β [see section 2b(1)].

[4] In an inviscid unforced atmosphere, mixing will be efficient at the surface, and the instability will be eliminated before all the tropospheric PV gradients are mixed.

[5] The PV gradient equals the meridional vorticity gradient minus the vertical derivative of density weighted isentropic slopes [see section 2b(1)].

study his suggested neutral state. It is important to understand the implications of the simplifications in these simple models on the stability characteristics of baroclinic waves in order to relate their results to the real atmosphere. The Charney model has no tropopause and has nonzero PV gradients in the troposphere. The Eady model has zero PV gradients in the troposphere and a tropopause, represented by a lid.

In the present study, we look at the neutralization mechanism proposed by Lindzen (1993) using a variety of more realistic but still simple models. The main goals are to study the effects of relaxing some of the major simplifications on the stability characteristics of normal modes and on the transition to a neutral state when the tropopause is lifted. Our studies also allow us to comment on the relative importance of wind and Brunt–Väisälä frequency on the stability characteristics of the waves.

The two main simplifications of the Eady model, which we relax, are the following:

1) The effect of replacing the lid by a more realistic tropopause and stratosphere. This part of the study has broader implications than for neutralization theory because it confirms the relevance of an Eady model to unbounded atmospheres.
2) The effect of having some small but nonzero PV gradients. Models show us that the presence of some PV gradients in the troposphere affects the stability characteristics considerably. The case where PV gradients are equal to the planetary vorticity gradient has been checked by Charney (1947) and Green (1960) and it is known that there is no short-wave cutoff, hence no neutral state as suggested by Lindzen (1993). It is therefore of interest to check how the stability characteristics change as the PV gradients are varied from zero to β. There is no reason to expect that decreasing the PV gradients will converge smoothly toward neutrality. On the contrary, the neutralization through the Charney–Stern criterion is such that the growth rates do not become small until a state very close to neutral is reached (Snyder and Lindzen 1988; Lindzen and Farrell 1980a).

b. Outline of the experiments

We start out by studying the stability characteristics of different one-dimensional (vertical) basic states. Two situations are considered. One is a ''troposphere–stratosphere'' model, which has a troposphere, tropopause, and a stratosphere. The second one is a simplified model in which a lid is placed at the tropopause. It is used to study the effects of replacing the lid in the classical models by a more realistic unbounded atmosphere structure. For each type of model several runs are made. Each run consists of calculating the normal modes and dispersion relations for 11 different profiles, which differ from each other in the tropospheric value of PV gradients. We then proceed to do a third set of runs, which consists in changing the height of the tropopause in the troposphere–stratosphere model while keeping PV gradients zero in the troposphere, to check what effect lifting the tropopause has on the short-wave cutoff.

Section 2 describes the model and the calculation of the basic states. Section 3a discusses the effect of replacing the lid by a tropopause and stratosphere, and the effects of having nonzero PV gradients. In section 3b we describe the effect of raising the tropopause and discuss the relative importance of wind and temperature profiles in this context. The conclusions are reviewed in section 4. The numerical procedure is described in the appendix.

2. The model

a. The equations

The quasigeostrophic equation of conservation of pseudo potential vorticity (PV) linearized around a zonal-mean basic state is used. The formulation mostly follows Lindzen (1994a):

$$\left(\frac{\partial}{\partial t} + U\frac{\partial}{\partial x}\right)q' + v'\frac{\partial \overline{q}}{\partial y} = 0, \tag{1}$$

where q', $\overline{q}$ are the perturbation and zonal-mean PV:

$$q' = \frac{1}{f_0}\left(\frac{\partial^2\phi'}{\partial x^2} + \frac{\partial^2\phi'}{\partial y^2}\right) + e^{z/h}\frac{\partial}{\partial z}\left(\frac{f_0^2}{N^2}e^{-z/h}\frac{\partial\phi'}{\partial z}\right) \tag{2}$$

$$\frac{\partial \overline{q}}{\partial y} = -\frac{\partial^2 U}{\partial y^2} + \beta - e^{z/h}\frac{\partial}{\partial z}\left(\frac{f_0^2}{N^2}e^{-z/h}\frac{\partial U}{\partial z}\right), \tag{3}$$

where x, y, z, and t are the zonal, meridional, height, and time coordinates respectively; ϕ is the geopotential streamfunction. The basic-state zonal wind, U, is taken to be independent of y; N is the Brunt–Väisälä frequency, given by

$$N^2 = \frac{g}{\theta_s}\frac{d\theta_s}{dz} = \frac{g}{T_s}\left(\frac{dT_s}{dz} + \frac{g}{c_p}\right);$$

h is the density scale height, which is assumed constant.

The boundary conditions are a rigid surface at the bottom and a radiation condition applied at the top of the stratosphere (at six scale heights). At a rigid surface the vertical velocity is set to zero in the thermodynamic equation:

$$\left(\frac{\partial}{\partial t} + U\frac{\partial}{\partial x}\right)\theta' + v'\frac{\partial \overline{\theta}}{\partial y} = 0. \tag{4}$$

A radiation condition is invoked by requiring the solution to vanish at ∞.

The perturbations are assumed to have a sinosodial horizontal structure with a zonal complex phase speed c:

$$\phi'(z) = \varphi'(z)e^{i\cdot k(x-ct)+i\cdot ly}, \quad (5)$$

where k, l are the zonal and meridional wavenumbers, respectively.

The equations are nondimensionalized in the following way (nondimensional variables are denoted by a tilde):

$$\tilde{z} = \frac{z}{H}$$

$$(\tilde{k}, \tilde{l}) = (k, l)L$$

$$\tilde{U} = \frac{U - U(0)}{U_T}$$

$$\tilde{c} = \frac{c - U(0)}{U_T}$$

$$\tilde{\phi} = \frac{\phi}{U_T f_0 L}$$

$$\tilde{\theta} = \frac{gH}{U_T f_0 L}\theta$$

$$\tilde{T} = \frac{T}{T_0}, \qquad T_0 \equiv T(z = 0)$$

$$\frac{d\tilde{T}}{d\tilde{z}} = \frac{H}{T_0}\frac{dT}{dz}$$

$$\tilde{N}^2 = \frac{N^2}{N_0^2}$$

$$\tilde{q}_y = \overline{q}_y \frac{H^2 N_0^2}{U_T f_0^2}. \quad (6)$$

For brevity, we remove the tildes and denote dimensional variables by asterisks.

The following relations are used: $\theta' = \partial\phi'/\partial z$, $\overline{\theta}_y = -U_z$ (thermal wind balance), and $v' = \partial\phi'/\partial x$.

The resulting nondimensional equations are

$$\frac{\partial}{\partial z}\left(\frac{e^{-zb}}{N^2}\varphi_z\right) + e^{-zb}\left(\frac{\overline{q}_y}{U - c} - \mu^2\right)\varphi = 0 \quad (7)$$

$$\frac{\partial\varphi}{\partial z} - \frac{U_z}{U - c}\varphi = 0 \quad \text{at } z = 0. \quad (8)$$

The nondimensional parameters are $\beta_e \equiv (\beta H^2 N_0^2)/(U_T f_0^2)$ [Eq. (12)], $\mu \equiv KHN/f_0$ ($K = \sqrt{k^2 + l^2}$), and $b \equiv H/h$. In all runs except when the Boussinesq approximation is made, $b = 1$. For a Boussinesq fluid the scale height (h) is effectively infinite, which implies $b = 0$.

To implement a radiation condition at the top, wind and temperature are held constant at the top scale height of the atmosphere. A transformation of variables is made:

$$\varphi = e^{(b/2)z}\sqrt{N^2}\psi. \quad (9)$$

This puts the equation in canonical form. Taking into account that N^2 is constant at the top, the solution becomes analytically tractable and has the form of a superposition of an upward and downward propagating wave. Only the upward propagating part is chosen. The solution is then transformed back into our original variable φ:

$$\varphi_z + \left(-\frac{b}{2} + in_{\text{ref}}(c)\right)\varphi = 0 \quad \text{at } z = \text{top}, \quad (10)$$

where

$$n_{\text{ref}} = \sqrt{-\mu^2 N^2 - \frac{b^2}{4} + \frac{N^2\overline{q}_y}{U - c}} \quad (11)$$

and we choose the square root that yields $\text{Im}(n_{\text{ref}}) \geq 0$.

Standard values are used for the different parameters: $U_T = U^*(z^* = H) = 22$ m s^{-1}, $T_0 = 285$ K, $N_0^2 = 1.1 \times 10^{-4}$ s^{-2}, $H = 8.9$ km, $\beta = 1.6 \times 10^{-11}$ s^{-1} m^{-1}, and $\beta_e = 0.64$; L is chosen to be the radius of deformation; $L^2 = N_0^2 H^2/f_0^2$. Unless specified differently, the tropopause is taken at $z = 1$, that is, at 8.9 km. The top of the troposphere–stratosphere model is chosen at $z = 6$ (53.5 km).

For a given wavenumber (μ), the equations are solved as an eigenvalue problem for c, where φ is the corresponding eigenvector. The numerical algorithm is explained in the appendix.

b. *The vertical profiles of basic-state PV, wind, and temperature*

The basic-state specification is divided into two parts: First, the PV gradient is specified in the troposphere and wind and temperature are calculated from it. Second, shear and vertical temperature gradients are specified in the stratosphere and the PV gradient is calculated from them. The two regions are matched to keep wind and temperature continuous.

This method of specifying the basic states in the troposphere and stratosphere separately and matching across the tropopause is chosen for convenience. In the troposphere, PV gradient is the most important basic-state quantity for the stability characteristics. It is best to specify it and calculate the wind and temperature from it. In the stratosphere, however, the basic state is determined also by other processes, and it is much easier to specify wind and temperature and calculate PV gradient rather than do the opposite. The reason for this will be explained in section 2b(2).

The calculations are done following Lindzen (1994a).

1) CALCULATING WIND AND TEMPERATURE FROM A SPECIFIED PV DISTRIBUTION

The PV profile in the troposphere is varied gradually from a state of zero PV gradients everywhere to a state with gradients of β, in jumps of 0.1β. The state of zero

PV gradients will be referred to as the mixed state or profile.

Once the PV gradient is specified, consistent wind and temperature profiles can be calculated, given some assumptions on the partition of the adjustment between these two properties.

Nondimensionalizing the expression for the basic-state PV gradient yields

$$\overline{q}_y = \beta_e + b\frac{U_z}{N^2} + \frac{\partial}{\partial z}\left(\frac{U_z}{N^2}\right) = \beta_e - e^{zb}\frac{\partial}{\partial z}\left(e^{-zb}\frac{U_z}{N^2}\right). \quad (12)$$

Multiplying both sides of the equation by e^{-zb} and integrating over z yields

$$\frac{U_z}{N^2} = \frac{\beta_e}{b}(e^{zb} - 1) + \frac{U_z(0)}{N^2(0)}(e^{zb} - g) \quad (13)$$

$$g = \frac{N^2(0)}{U_z(0)}e^{zb}\int_0^z e^{-zb}\overline{q}_y\, dz \quad (14)$$

(for $b \neq 0$).

Given the vertical profile of $\overline{q}_y$ and the values of shear and static stability at the ground, the quantity U_z/N^2 at each height can be calculated. In most runs, $U_z(0)$ and $N^2(0)$ are chosen such that wind and temperature at the tropopause assume a certain characteristic value. The reason for this is to have a similar stratospheric basic state for profiles with different PV gradients in the troposphere (see next section). This choice of surface values is somewhat arbitrary. The sensitivity of the results to this choice will be discussed when relevant.

The partitioning between U_z and N^2 is also somewhat arbitrary. One possibility is to introduce a parameter α in the following way:

$$N^2 = \frac{N^2(0)}{[(\beta_e N^2(0)U_z(0) + 1)(e^{zb} - 1) - g]\alpha + 1}. \quad (15)$$

From Eqs. (15) and (13) it follows that

$$U_z = U_z(0)\frac{(\beta_e N^2(0)/U_z(0) + 1)(e^{zb} - 1) - g + 1}{[(\beta_e N^2(0)/U_z(0) + 1)(e^{zb} - 1) - g]\alpha + 1}. \quad (16)$$

The new parameter α is a measure of the partition of the PV distribution between the wind and temperature fields: $\alpha = 1$ means all the adjustment is done by the static stability, and $\alpha = 0$ means all the adjustment is achieved by the wind field. For standard runs $\alpha = 0.5$ is chosen. The same procedure can be followed for the Boussinesq case ($b = 0$). The wind profile is obtained by integrating U_z subject to $U(0) = 0$. The temperature can be calculated from N^2, assuming $T(0) = 1$ (in nondimensional units).

Figure 1 shows the resultant basic-state profiles. Note that the adjustment in U and T, required to change the PV gradient values from β to zero, is small. Observationally, it may be very hard to detect. This degree of similarity between the different wind and temperature profiles is a result of having wind and temperature values fixed at the tropopause. Different boundary specifications for shear and static stability may yield profiles that are not as similar.

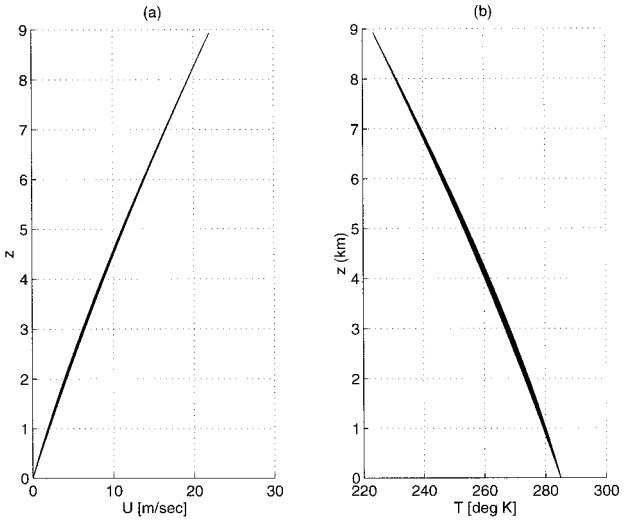

FIG. 1. Basic states for the different PV gradient profiles (see text for details). (a) Wind (in m s^{-1}). The ''mixed'' profile is on the left. (b) Temperature (in kelvins). The mixed is on the right.

2) CALCULATION OF THE UPPER-ATMOSPHERIC BASIC STATES

The basic-state wind shear and vertical temperature gradients are specified between the tropopause and 50 km. An approximation to a standard atmosphere is used, following Lindzen (1994a) (wherein details may be found). Above 50 km the wind and temperature are taken to be constant, to facilitate the implementation of a radiation condition. A basic assumption made is that the effect of the mesosphere on the stability characteristics of tropospheric waves is small. Some evidence of this is found in Kuo (1979).

Here U_z and T_z are specified to be the same above the tropopause in all runs. These are then integrated to obtain U and T, assuming continuity with tropospheric profiles. The resultant profiles have a discontinuity in the U_z and T_z fields at the tropopause. This causes very sharp spikes of PV because the PV operator includes differentiation. These spikes are artificially thin. A spline fit is imposed on the temperature and wind profiles in a narrow region around the matching point, to remove the spikes in $\overline{q}_y$. The results are found not to be sensitive to the width of this smoothing region.

Figure 2 shows the profiles that correspond to matching the stratospheric profiles above to the tropospheric profiles shown in Fig. 1. Note that the value of $\overline{q}_y$ at the tropopause increases as $\overline{q}_y$ in the troposphere is decreased, as expected from mixing a conserved quantity

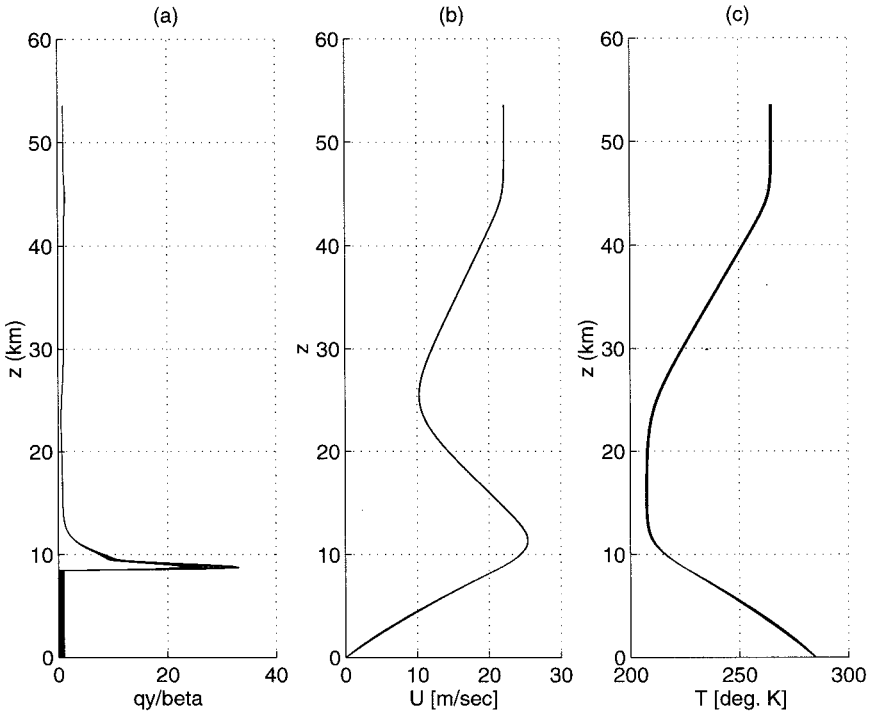

FIG. 2. The basic state for the different PV gradient profiles as prescribed in the troposphere–stratosphere models (see text for details): (a) PV gradients in units of β, (b) winds (in m s^{-1}), and (c) temperature (K). As in Fig. 1, the differences between the profiles are almost indistinguishable. The main differences are the constant value that the PV gradient assumes in the troposphere and the magnitude of the peak at the tropopause. The smaller the PV gradient is in the troposphere, the larger the maximum value is at the tropopause.

in a specific region (its gradients increase at the edge of the mixing domain). Mathematically, the reason for this behavior is the following.

Evaluating Eq. (13) at the top and using the fact that the shear at the top is zero yields the following constraint on $\overline{q}_y$:

$$\int_0^{\text{top}} e^{-zb}\overline{q}_y\, dz = \frac{\beta_e}{b}(1 - e^{-z_{\text{top}}b}) + \frac{U_z(0)}{N^2(0)}, \quad (17)$$

which means that the total atmospheric mass-weighted integral of $\overline{q}_y$ has to assume a specific value that depends on the isentropic slopes at the surface ($U_z(0)/N^2(0)$). Since the stratospheric basic states are designed to be identical for these profiles, it is easy to show that decreasing $\overline{q}_y$ in the troposphere will cause it to be increased at the tropopause. Equation (17) implies that $\overline{q}_y$ cannot be specified arbitrarily if we are to have vanishing isentropic slopes at the top.[6] It is therefore much easier to specify wind and temperature in the stratosphere and calculate $\overline{q}_y$ from them.

3. The model runs and results

a. The basic characteristics of the waves on basic states with a tropopause and a stratosphere

Figure 3 shows the dispersion relation for perturbations on the basic states shown in Fig. 2. The real and imaginary phase speeds are plotted as functions of total wavenumber, where the wavenumber is given in terms of the number of waves that fit into a latitude circle at 45°. When calculating the growth rates, kc_i, we need to specify the zonal wavenumber explicitly. We assume for simplicity that the meridional wavenumber is zero.

To simplify the discussion, we will refer to the profiles with $\overline{q}_y = \beta$ and $\overline{q}_y = 0$ as the Green model and Eady model profiles, respectively. These refer to the corresponding classical models when a lid is placed at the tropopause.[7]

The transition from the Green model modes to the

[6] Zero isentropic slopes at the top is a condition necessary for the implementation of a radiation condition. However, in the real atmosphere, the isentropic slopes are very small, which also imposes a strong restriction on the PV gradient profile.

[7] The Eady model actually refers to the modified Eady model (Lindzen 1994b; Grotjahn 1979), which is like the classic Eady model (Eady 1949) in that it has zero PV gradients, only instead of having $\beta = 0$ and constant shear and N^2, it has $\beta \neq 0$ and the wind and temperature are modified to render $\overline{q}_y = 0$. In the classical Green and Eady models, constant shear and N^2 are also assumed, as well as a Boussinesq fluid.

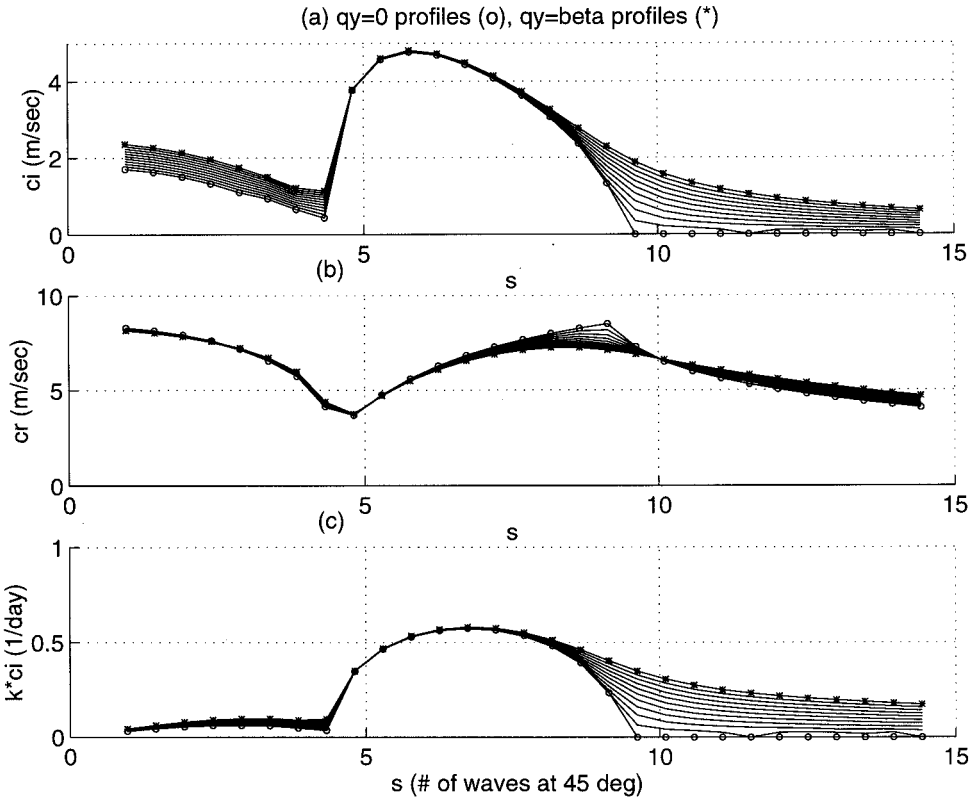

FIG. 3. Imaginary (a) and real (b) phase speeds (m s^{-1}) and growth rate (c) (day^{-1}) for the profiles shown in Fig. 1. The mixed profile is denoted by circles, the $\overline{q}_y = \beta$ profile by stars. Wavenumbers in (a) and (b) are total wavenumbers, in terms of the number of wavelengths that fit into a latitude circle at 45°. In (c) zero meridional wavenumber is assumed.

Eady model modes is smooth. This result is important for the neutralization theory to hold in more realistic cases. The short-wave growth rates in Fig. 3 gradually decrease from the Green model values of 0.2–0.3 day^{-1} to zero, to form the short-wave cutoff of the Eady model. There are two neutral short waves, a tropopause wave and a surface edge wave (only the surface wave branch of the phase speed is shown here). The convergence of the short waves as $\overline{q}_y$ is decreased is toward the surface edge waves. The unstable part of the dispersion relation is remarkably similar for the different profiles. The maximum growth rate is around 0.57 $days^{-1}$. This is consistent with the scaling arguments of Lindzen and Farrell (1980b).

Figures 4 and 5 show the vertical structures of pressure and temperature and the heat and PV fluxes of typical long, medium, and short waves, for the profile with $\overline{q}_y = 0$ in the troposphere.

The pressure perturbation of a rapidly growing (medium) wave has a peak at the surface and a slightly larger one at the tropopause. The phase tilts westward with height in the troposphere, as is required of a perturbation that is to draw energy from the mean flow. The temperature phase tilts slightly eastward with height in the troposphere, as expected from simple classical models. The medium wave temperature perturbation also has a peak in the lower stratosphere, which is as large as the tropospheric perturbation. Above that, the perturbation decays. The structure at the tropopause suggests a node; that is, there is a rapid phase shift with height of almost 180° associated with very small amplitude. This feature is consistent with having a maximum pressure perturbation at the tropopause. There are observations of perturbations with a similar structure in the atmosphere (Randel and Stanford 1985). Neutral surface short waves have a maximum pressure perturbation at the surface, which decreases monotonically upward in the troposphere. The meridional PV fluxes of all unstable waves are zero in the troposphere and peak at the tropopause. Correspondingly, the meridional heat fluxes of these waves decrease like density in the troposphere. Medium waves have negligible heat flux in the stratosphere. One of the new features of the troposphere–stratosphere model compared to the classical models is the existence of unstable long waves with large amplitudes in the stratosphere. These will be discussed later.

For comparison, the calculations are repeated with a lid at the tropopause ($z = 1$), using the same tropospheric profiles, for all the different runs that were done

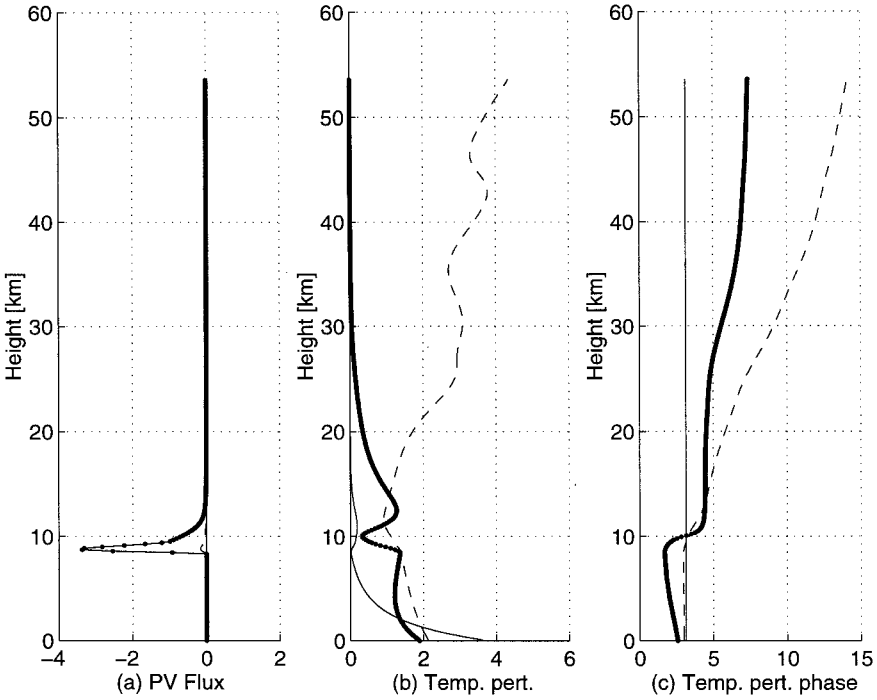

FIG. 4. Vertical structures of typical long (dash), medium (thick), and short (thin) waves: (a) PV fluxes $\rho\overline{v'q'}$, (b) temperature perturbation amplitudes, and (c) temperature perturbation phases (radians). Units in (a) and (b) are arbitrary.

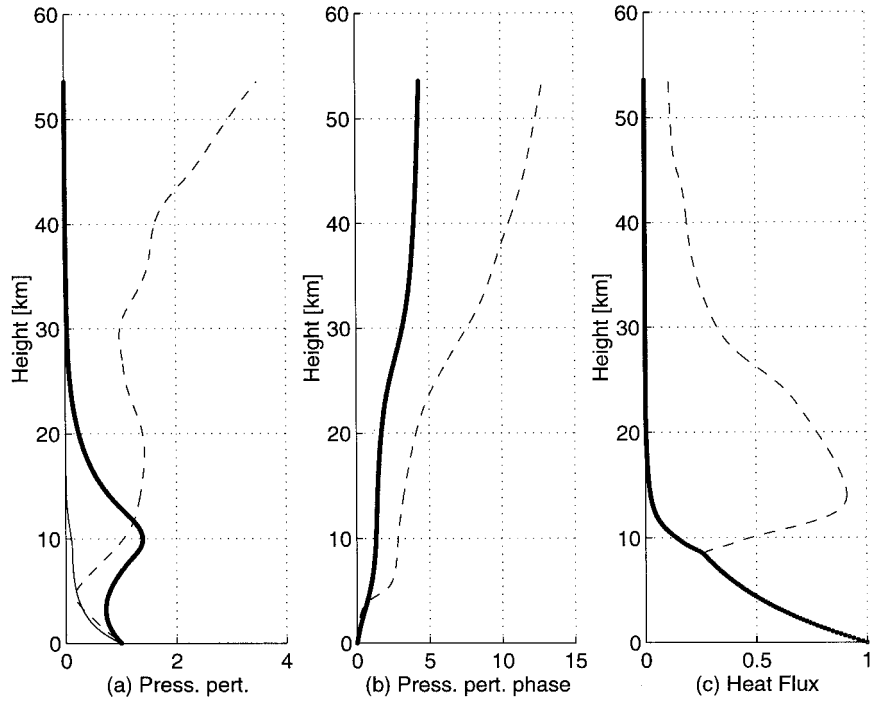

FIG. 5. Vertical structures for the same waves as in Fig. 4: (a) pressure perturbation amplitudes, (b) pressure perturbation phases (radians), and (c) heat fluxes $\rho\overline{v'T'}$. Units in (a) and (c) are arbitrary.

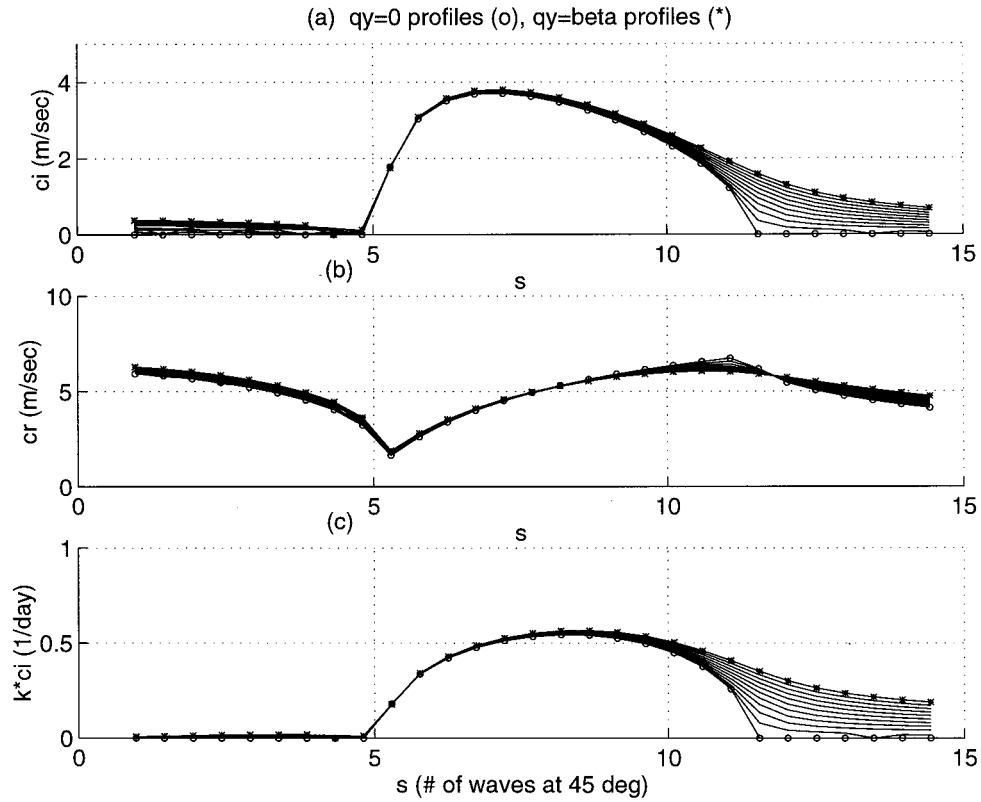

FIG. 6. As in Fig. 3 only for the lid basic states shown in Fig. 1.

with the troposphere–stratosphere model. The dispersion relations obtained (Fig. 6) are qualitatively similar to the troposphere–stratosphere models in many aspects, with a few significant differences.

The one most relevant to the current discussion is a shift of the short-wave cutoff to smaller wavelengths. This is a very robust feature. Each run with the lidded models yields a cutoff at larger wavenumbers than its more realistic troposphere–stratosphere counterpart. The shift is typically 2–3 wavenumbers. The cutoff values for the lidded model runs are all in the range of wavenumbers 10–15, whereas the ''realistic'' models have cutoffs at wavenumbers in the range of 8.5–10.

A simple scaling analysis shows that the average vertical decay rate of an Eady edge wave is proportional to $\langle N \rangle \mu$, where $\langle N \rangle$ is the tropospheric average of N and μ is the horizontal wavenumber (see section 3b). When $\langle N \rangle$ and the short-wave cutoff for many different runs of the model with a lid are plotted together, a linear relation between the two emerges. The larger $\langle N \rangle$ is, the more rapidly the waves decay away from the surface and the smaller the short-wave cutoff is. This suggests that this cutoff forms when the surface and top edge waves are too shallow to affect each other and interact.

The model with a tropopause and a stratosphere shows a strong correlation between $\langle N \rangle$ and the short-wave cutoff, which is pretty linear, but not all runs follow it exactly. Since the tropospheric profiles are identical by construction in the two models (with and without a lid), some factors other than the average tropospheric static stability are important in determining the cutoff.

It is likely that in the realistic model, some destructive interference of the wave in the tropopause waveguide makes the mutual interaction harder, especially for waves that are only weakly interacting in the ''lid'' model (i.e., waves that are slightly longer than the short-wave cutoff). A similar interference mechanism was suggested by Lindzen et al. (1980) to be the cause of the neutral points in the Charney model.

The vertical structures suggest the same. While the lower-tropospheric structures are relatively similar in both types of models, there are interesting features at the tropopause and lower stratosphere for the unbounded model. The temperature perturbation of the surface short wave decays to zero at the upper troposphere but it has a secondary peak of temperature perturbation in the lower stratosphere (Fig. 4). It seems as if the surface edge wave does manage to ''tunnel'' through the troposphere into the tropopause waveguide, but not enough for mutual reinforcement. The tropopause short wave (not shown), on the other hand, has a large pressure perturbation peak at the tropopause and a small perturbation at the surface. This wave, too, manages to reach the surface. It seems as if there is some minimum amount

of tunneling needed for the surface and tropopause waves to phase lock and grow.

The shift in the short-wave cutoff moves the whole spectrum such that the most unstable modes have smaller wavelengths in the lid runs. The long-wave cutoff also shifts in some of the runs, although not in all of them. This raises the question of what happens when the tropopause is lifted and the short-wave cutoff reaches the long-wave cutoff. This will be discussed in the next section.

The second major effect of putting a lid at the tropopause is on the structure and growth rate of long waves, which tend to be deeper than the troposphere. Unlike the medium and short waves, which have similar growth rates in the lid and troposphere–stratosphere models, the long waves are effectively neutralized by the presence of a lid. They are neutral for the Eady profile[8] and grow very slowly when some internal PV gradients are present. This result is expected. Green (1960) found that putting a lid at the tropopause in the Charney model stabilizes the long waves considerably.

It is actually interesting that the growth rates of the long waves in the troposphere–stratosphere models are not larger than they are. In the Charney model the long waves have quite large growth rates but their structure is of an edge wave, which decays away from the surface. In the present model, the long waves grow much more slowly than Charney modes but they have large amplitudes in the stratosphere. They do not seem to be affected by the value of PV gradients in the troposphere. The difference therefore from the Charney model lies in the existence of a tropopause, that is, a region of very large PV gradients. The large amplitudes in the stratosphere depend on the wave being able to propagate upward there. The stratospheric region, which has nonzero PV gradients, acts as a wave propagation region for waves longer than a certain wavelength (Charney and Drazin 1961). The transmission properties of the waves depend on the stratospheric index of refraction, which is a strong function of the PV gradient, the phase speed, and the zonal wind. Most important, there may be critical layers in the stratosphere that could make a qualitative difference for the structure of these deep modes. Since we can specify a given PV gradient profile using different wind profiles, it is plausible to have different deep modes for the same $\overline{q}_y$. One complication is dependence of the index of refraction on the phase speed, which is part of the solution. It is possible that the phase speed will vary to keep the index of refraction fairly similar for these different profiles. It is unclear to what extent the stratosphere controls the phase speed of the modes. In any case, the effect of the stratosphere is expected to be smaller for medium and short waves that are confined to the troposphere than for deep long waves.

This brings us to the following point: the design of this experiment assumes that the physical property that matters most for the stability characteristics is the PV gradient and that the role of temperature and wind individually is small. This assumption has to be made in order to justify the approach in which the PV gradient is specified and wind and temperature are calculated from it somewhat arbitrarily. The validity of this assumption is tested to some extent by varying α in Eqs. (16) and (15), or by specifying the values of static stability or wind at the ground in several different ways. Results of repeating the experiment with different values of these constants, as well as relaxing the Boussinesq approximation, leave us with the following picture: the robust features of the results described above are the gradual transition to a short-wave cutoff for the Eady model and the convergence of the real phase speed to the lower Eady mode. The striking similarity of the dispersion relations at medium and long wavelengths disappears for many of the runs. The differences, however, are only quantitative. Qualitatively, they are similar. It is hard to isolate the effect of different features of the wind and temperature profiles. The only strong relation we found is the correlation between $\langle N \rangle$ and the short-wave cutoff. The features that are sensitive to details of the wind and temperature profiles in the lid model runs are sensitive in the troposphere–stratosphere runs as well. We will discuss this issue further in the next section.

b. Lifting the tropopause

Lindzen (1993) estimated roughly that the required tropopause height to neutralize even the longest waves would be about 16 km for a typical jet width. This estimate is based on the classical Eady model. D. Kirk-Davidoff (1996, personal communication) improved the estimate by using a modified Eady model (see Fn 7) in which the effect of β and density changes with height were included. He found a strong dependence on how one specifies static stability. Profiles that yield the observed tropospheric vertical average of N result in reasonable tropopause heights. However, these profiles had too large a value of static stability at the ground, especially for a high tropopause. Profiles with the observed values at the ground but too low a tropospheric average were not neutralized for lids at even 20 km.

Results of the previous section motivate checking specifically for the effect of replacing the lid by a more realistic tropopause on the neutralization mechanism through the Eady model short-wave cutoff. There are several reasons for doing this:

[8] Long waves are neutral in the modified Eady model. In the classical Eady model they are unstable. The reason they are not inhibited by a lid at the tropopause is that the waves are edge waves and not internal Rossby waves, as in the Green model. The stability of long waves in the modified Eady model appears to be related to the inability of the two edge waves to phase lock in the presence of β.

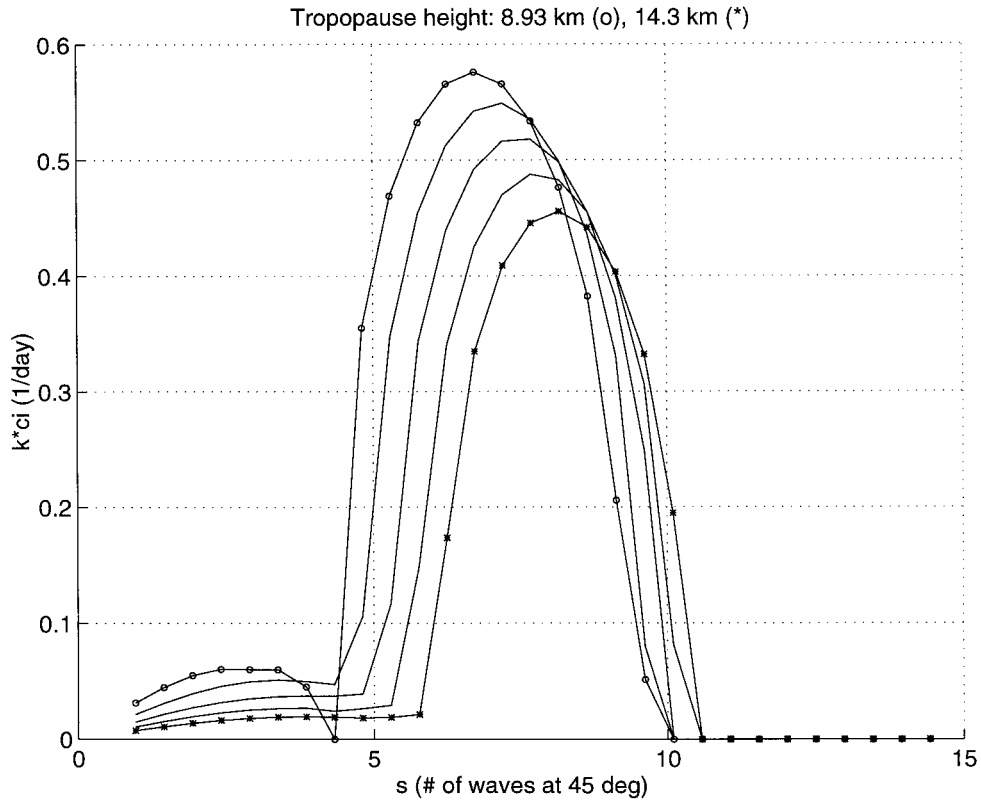

FIG. 7. The growth rates (day^{-1}) for five different basic states corresponding to different tropopause heights, with the same tropospheric vertical integral of N. Circles correspond to a tropopause height of 8.93 km and stars to 14.3 km.

1) The short-wave cutoff moves to longer wavelengths in the more realistic model. This suggests it may be easier to neutralize the atmosphere because less tropopause lifting will be required to reach the neutral cutoff. On the other hand, results suggest that other factors, apart from average N^2, determine the short-wave cutoff; in particular, there is possibility for destructive interference in the tropopause region. It is therefore not obvious that the short-wave cutoff will move in the same way as in the ''lid'' models. This is especially true since lifting the tropopause causes it to sharpen and change its shape.
2) An interesting question is what happens when the short-wave cutoff gets very close to the long-wave cutoff. Does the long-wave cutoff move to even longer wavelengths or does the range of rapidly growing wavenumbers decrease until it is eliminated completely? In the latter case, the tropopause height will be lower than that implied by moving the short-wave cutoff to the minimum meridional wavenumber.
3) The differences between the wind and temperature profiles resulting from the various ways of dividing the PV gradient structures between the two become very large when the tropopause is high. We may use this to study the sensitivity of the normal modes to quantities other than the PV gradient.

The eigenvalue problem is solved again for the case where PV gradients are zero in the troposphere, but now the tropopause is raised gradually such that the height at which the atmosphere will become effectively neutral can be found. Assuming a jet width of $0.15a$ (a is the radius of the earth), as was assumed by Lindzen (1993), implies a minimum meridional wavenumber of about 4.7. This means that the model atmosphere is effectively neutral when the short-wave cutoff reaches a wavenumber of about 4.7.

In the previous section we mentioned the relationship between the short-wave cutoff and $\langle N \rangle$. We will further test it here. Transforming Eq. (7) into canonical form using Eq. (9), we get

$$\psi_{zz} + \left(-\mu^2 N^2 - \frac{1}{4} - \frac{1}{2}\frac{(N^2)_z}{N^2} + \frac{1}{2}\frac{(N^2)_{zz}}{N^2} - \frac{3}{4}\left(\frac{(N^2)_z}{N^2}\right)^2 + \frac{N^2 \overline{q}_y}{U - c}\right)\psi = 0. \tag{18}$$

The WKB solution in the troposphere, where $\overline{q}_y = 0$, is approximately of the form (assuming N^2 changes slowly in the troposphere):

$$\varphi \propto \varphi(0) e^{\pm \mu \int_0^z N\, dz}, \tag{19}$$

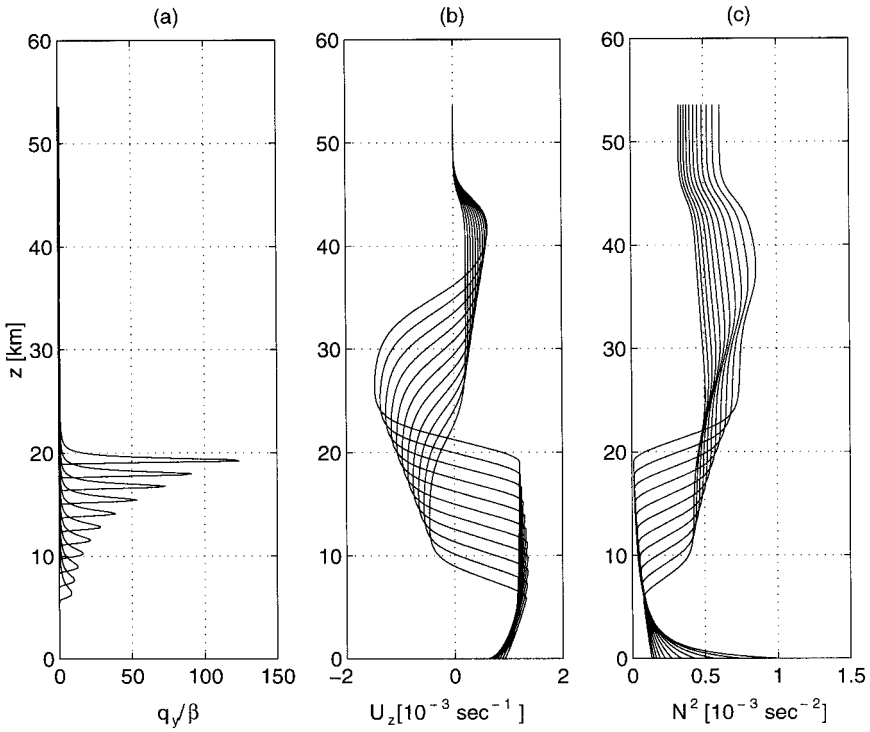

FIG. 8. The basic states for different tropopause heights (6.25–19.65 km). See text for details. (a) PV gradients in units of β; (b) wind shear (m s^{-1}/km); and (c) Brunt–Väisälä frequency N^2 (10^{-3} s^{-2}).

where the minus (plus) in the exponent corresponds to the surface (tropopause) edge wave. The fractional amount of surface wave that reaches the tropopause is proportional to $e^{-\mu\int_0^{z_t} N dz}$, where z_t is the height of the tropopause. If the short-wave cutoff forms when the amount of tunneling becomes smaller than some number, it will be inversely proportional to $\int_0^{z_t} N\,dz$. In the Eady model, this is equal to NH.

We test this relation by lifting the tropopause while keeping the integral of N in the troposphere constant. Figure 7 shows the growth rates for five different tropopause heights. We see that the short-wave cutoff shifts very little (cf. Figs. 9–11). There is actually a very slight shift to shorter waves as the tropopause is raised. We conclude from this run that there is a minimum amount of tunneling of the waves between the surface and tropopause needed for them to mutually interact and grow. Waves that are too short will be neutral. In order to keep the tropospheric integral of N constant as we lift the tropopause, we need to decrease the tropospheric average of N^2 to unrealistic values (0.18 s^{-2} for a tropopause at 14.3 km). It is unlikely this is what the atmosphere will do.

Special attention should be given to the specification of boundary shear and N^2. Raising the tropopause implies, as a rule, increasing the region in which $\overline{q}_y = 0$. From Eq. (13) the isentropic slope at the top of the $\overline{q}_y = 0$ region (z_t) is

$$\mathrm{IS}(z_t) \equiv \frac{U_z}{N^2}(z_t) = e^{z_t b}\left(\frac{\beta_e}{b} + \frac{U_z(0)}{N^2(0)}\right) + \frac{\beta_e}{b}. \quad (20)$$

The higher the tropopause (larger z_t), the more sensitive IS(z_t) is to the value of isentropic slopes at the surface. For example, if we keep U_z and N^2 constant at the surface as we lift the tropopause, the value of the isentropic slopes at the tropopause will increase exponentially with the height of the tropopause. On the other hand, if we keep tropopause isentropic slopes the same, the surface value has to decrease exponentially with tropopause height. Accordingly, the difference in wind and temperature profiles between these two cases is larger, the higher the tropopause. Since it is unclear how the atmosphere will behave as the tropopause is pushed upward, we test a few possibilities. Our approach is to keep important atmospheric physical properties at observed values as the tropopause is raised.

In the first case the tropospheric average of N^2 and U_z (equator to pole temperature gradient) are kept constant. Figure 8 shows the resulting profiles. The most notable feature is the large increase in surface N^2 as the tropopause is raised. Also, the surface shear decreases. The value of $U_z(0)/N^2(0)$ is of utmost importance to the stability of the flow because it is equivalent to a negative spike of PV gradient at the surface (Bretherton 1966). If this negative spike is erased, either by decreasing U_z to zero or increasing N^2 to ∞, the PV gradients are

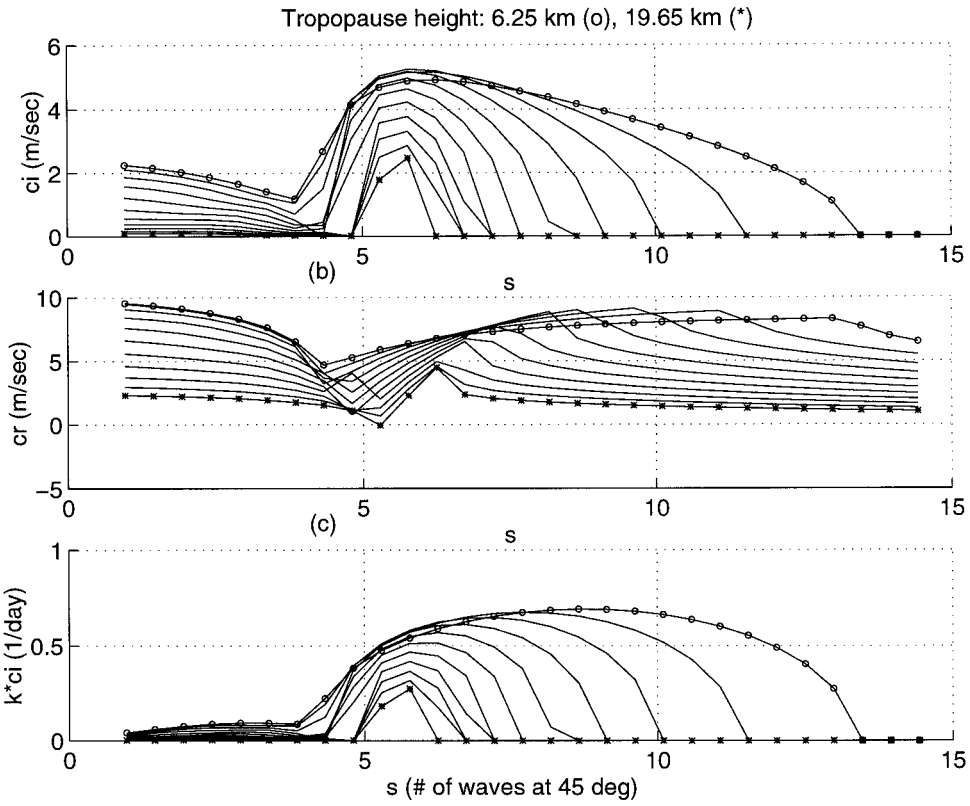

FIG. 9. As in Fig. 3 but for the dispersion relations for the profiles in Fig. 8. Circles correspond to a tropopause height of 6.25 km and stars to 19.65 km.

positive everywhere and the model atmosphere is stable (Charney and Stern 1962). The dispersion relation for these profiles is shown in Fig. 9. The short-wave cutoff gradually moves to longer waves as the tropopause is raised because the vertical integral of N increases, reaching wavenumber 6.25, at 19.6 km. At the same time the growth rates of the most unstable waves decrease rapidly, but only down to about 0.2 day^{-1}. When the tropopause is lifted enough, the increase in N^2 at the surface affects the growth rates. We are seeing a stabilization of the flow by the mechanism suggested by Gutowski (1985). The value $N^2(0)$ assumed in these runs is unrealistically high.

To avoid increasing N^2 at the surface, we keep it constant and make all the changes in the wind field, keeping the average shear constant (i.e., $\alpha = 0$). This results in a decrease of surface shear to negative values, and a corresponding stabilization. As explained in the introduction, wiping out the surface shear is not the neutralization method we are trying to check here.

To avoid stabilizing the flow through the Charney–Stern criterion, we repeat the run keeping U_z and N^2 constant at the surface. The resultant profiles have a decreasing tropospheric average of N^2 for increasing tropopause height. The integral of N increases more slowly than in the previous case, and only to a certain point, because the values of N in the upper troposphere become very low. Accordingly, the short-wave cutoff changes more slowly and eventually stops moving at wavenumber 8.2 for a tropopause at 22.3 km (Fig. 10). The growth rates increase slightly. This may be due the increase in $\overline{q}_y$ at the tropopause as it is lifted.

The current method of splitting adjustment of $\overline{q}_y$ between the winds and temperature profiles forces us to choose only two quantities to be held at observed values. Since this division is arbitrary, we choose a different one with one more degree of freedom and keep $N^2(0)$, $\langle N^2 \rangle$, and $U_z(0)$ at observed values; N^2 in the troposphere is specified as follows:

$$N^2 = N^2(0) \times \frac{\cosh\left(\dfrac{z - z_d}{\epsilon}\right)}{\cosh\left(\dfrac{z_d}{\epsilon}\right)}. \tag{21}$$

Here U_z is calculated from Eq. (13), and z_d and ϵ are chosen to give observed values of $\langle N \rangle$ and $U_z(0)$. Note that we cannot simultaneously control $\langle U_z \rangle$.

Figure 11 shows the dispersion relations for these

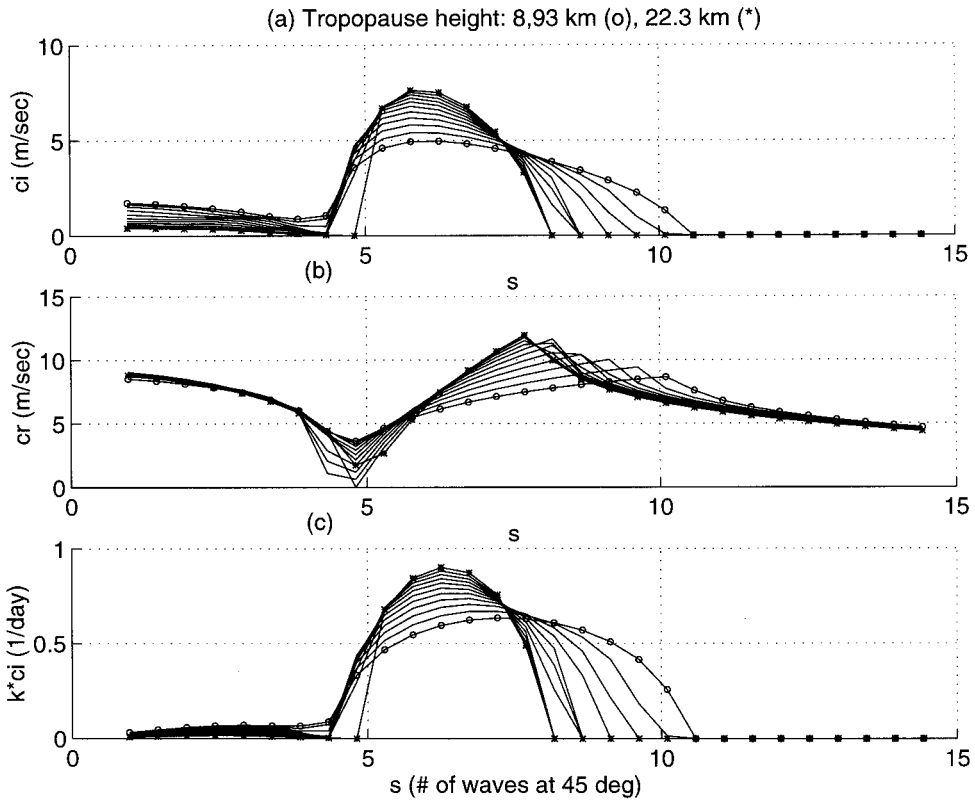

FIG. 10. As in Fig. 9 but for the case where wind shear and N^2 are kept constant at the surface. See text for details.

basic states. This time, the atmosphere is neutralized for a tropopause height of 18.3 km. However, the winds are unrealistically high for this state (maximum of 183 m s^{-1} at 21 km). This is due to $\langle U_z \rangle$ increasing as the tropopause is raised. It may well be that this does not matter for the short-wave cutoff formation for the following reason: U_z comes into the equations only at the surface boundary condition. Otherwise, it has an indirect effect by determining the values of wind. The only place wind comes into the equations, apart from the surface boundary condition, is through the term $\overline{q}_y/(U - c)$, which is part of the index of refraction. In the troposphere, which is the important region for the short waves, $\overline{q}_y$ is zero, so this term drops out. In the stratosphere, however, when U increases, $\overline{q}_y/(U - c)$ becomes very small. This causes the index of refraction in the stratosphere to become negative for longer waves. In other words, the larger the winds, the longer the waves have to be to propagate up into the stratosphere, by the Charney–Drazin criterion (1961). The result is that long waves have an index of refraction structure like the medium waves do when the tropopause is at $z = 1$. Correspondingly, they have large growth rates and vertical structures characteristic of medium waves and not long waves (as in Figs. 4 and 5).

The conclusions from these runs are ambiguous. What matters most for the short-wave cutoff is how much wave tunneling there is between the surface and the tropopause. This depends on the vertical tropospheric integral of N. Under realistic conditions, it changes in a way that will cause the short-wave cutoff to move to longer waves as the tropopause is raised. How much it will shift depends on the the way the mixing of PV is divided up between the wind and temperature fields.

It seems hard to construct basic states with zero PV gradients in the troposphere, and realistic surface values and tropospheric averages of both U_z and N^2, when the tropopause is high. It is unclear whether this is a result of oversimplifying the profiles of N^2 and U_z or an inherent problem the system has with wiping out the PV gradients in very large regions. In reality, of course, the atmosphere does not reach a strictly neutral state: $\overline{q}_y$ is not identically zero everywhere and the tropopause is lower than 18 km.

4. Conclusions

The results for the Eady model are shown to hold qualitatively when the lid is replaced by a relatively realistic tropopause and stratosphere. This is crucial for

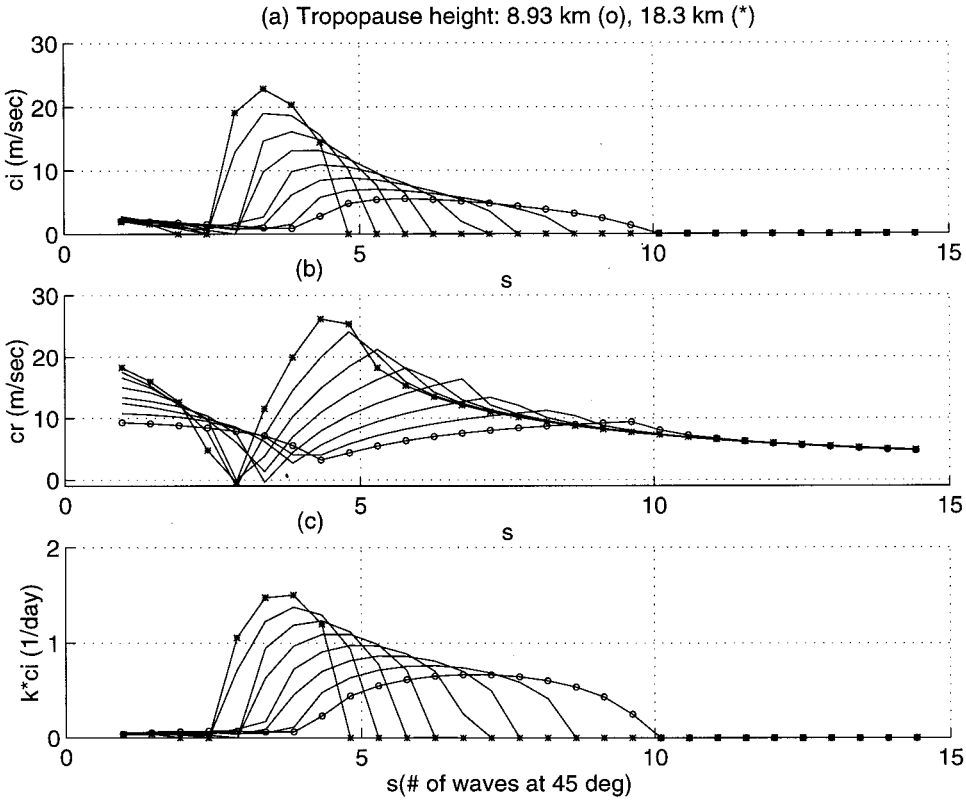

FIG. 11. As in Fig. 9 but for the case where surface wind shear and N^2 and the tropospheric average of N are kept constant. Circles correspond to a tropopause height of 8.93 km and stars to 18.3 km. See text for details.

Lindzen's (1993) neutralization theory to hold. As in the Eady model, the unstable modes are basically an interaction between a surface edge wave and a tropopause wave. The tropopause acts as a waveguide, wherein there can be interference of the modes, thus complicating the interaction of the surface and tropopause waves. In particular, the internal tropopause structure affects the formation of the short-wave cutoff; it shifts to longer wavelengths when the lid is replaced by a tropopause.

The more realistic tropopause and stratosphere basic state affects the long waves greatly; in particular, these waves can develop large stratospheric structures. This is a matter of independent interest and is being pursued further.

The transition from basic states with no tropospheric PV gradients to states with PV gradients on the order of β is smooth in phase speed space. The maximum growth rate is about the same for all PV profiles. The part of the spectrum that interests us most for the question of neutrality are the short waves. There is a gradual convergence of the growth rate curves toward neutrality, for waves beyond the short-wave cutoff. This means that even in the presence of small PV gradients, there may be an effective short-wave cutoff because the growth rates are smaller than damping rates. The possibility of neutralizing the flow is not dependent on the PV gradients vanishing identically, which is an unrealistic expectation; instead, the PV gradients have to be sufficiently small. Hence, the theory may apply to the real atmosphere, not just to a highly idealized one.

The results in general show that the PV gradient is the basic-state property that is dynamically most important for the stability characteristics. The direct effect of wind and temperature structures, for a given PV structure, is quantitative, not qualitative. This result was also found by Fullmer (1982a,b). He found that small changes in wind profiles affected the stability properties of his model greatly when the changes in wind were accompanied by large or qualitative changes in $\overline{q}_y$ (i.e., changing it from negative to positive values). When the small changes in wind were not accompanied by great $\overline{q}_y$ changes, the stability properties were little affected.

However, as the tropopause is raised, the sensitivity of the wind and temperature profiles (for a given PV gradient structure) to boundary specification of N^2 and U_z increases because PV is mixed in a larger domain. Differences between the profiles may have a large effect on the stability characteristics. Most important for the

neutralization studies is a difference in how the short-wave cutoff shifts as the tropopause is raised.

The following relations emerge from our results. The tropospheric vertical integral of N is important for the formation of the short-wave cutoff because it determines how much tunneling there is between the surface and tropopause waves. Also important are the values of shear and static stability at the surface because they determine the magnitude of the negative PV gradients at the surface. If this is zero or very small, the atmosphere becomes neutralized through the Charney–Stern criterion. When the tropospheric average and surface N^2 and U_z are held at observed values, the short-wave cutoff reaches a wavenumber typical of a meridional confinement due to the jet stream when the tropopause is at 18 km. However, at this state, the average tropospheric shear is much larger than observed. The tropospheric average of shear seems to be important when winds become very large in the stratosphere, affecting the propagation of long waves by the Charney–Drazin condition.

Our simple calculations suggest that it is hard to find realistic profiles that have zero PV gradients all the way up to a tropopause that is high (around two scale heights). This fact is interesting because it suggests some indirect constraint on the atmosphere and the effects of the eddies. It is important to remember in this respect that the atmosphere will not reach a strictly neutral state in the presence of dissipation and forcing. Small PV gradients in the troposphere and a tropopause lower than neutral can make it much easier to find realistic profiles.

Acknowledgments. The first author would like to thank especially Peter H. Stone for the discussions on this work, and to thank Gerard Roe, Daniel Kirk-Davidoff, and Amy Solomon for their discussions and help with the numerics. This work was supported in part by Grants NAG5-1328 from NASA, 914441-ATM from the National Science Foundation, and NAGW 525 from NASA. Ten percent of this research was funded by the U.S. Department of Energy's (DOE) National Institute of Global Environmental Change (NIGEC) through the NIGEC Northeast Regional Center at Harvard University (DOE Cooperative Agreement No. DEFC03-90ER61010) and through CHAMMP. Financial support does not constitute an endorsement by DOE of the views expressed in this article.

APPENDIX

The Numerical Calculations

The formulation is a variation on Snyder and Lindzen (1988). In general, the problem has the following form:

$$\frac{\partial(A(z)\psi_z)}{\partial z} + A(z)B(z, c)\psi = 0 \tag{A1}$$

with boundary conditions of the form

$$\psi_z + a(c)\psi = 0 \quad \text{at } z = 0 \tag{A2}$$

$$\psi_z + b(c)\psi = 0 \quad \text{at } z = \text{top}. \tag{A3}$$

These equations are then finite differenced in the following way:

$$(A\psi_z)_{zj} = \frac{(A\psi_z)_{j+1/2} - (A\psi_z)_{j-1/2}}{\Delta},$$

$$A_{j+1/2} = \frac{A_{j+1} + A_j}{2}, \quad \text{and} \quad \left(\frac{\partial\psi}{\partial z}\right)_{j+1/2} = \frac{\psi_{j+1} + \psi_j}{\Delta}.$$

Substituting into the equation above yields

$$\frac{A_{j+1} + A_j}{2}\psi_{j+1} + \left(2\Delta^2 B_j A_j - \frac{A_{j+1} + 2A_j + A_{j-1}}{2}\right)\psi_j + \frac{A_j + A_{j-1}}{2}\psi_{j-1} = 0 \tag{A4}$$

$$\psi_2 + 2\Delta a\psi_1 - \psi_0 = 0 \tag{A5}$$

$$\psi_{N+1} + 2\Delta b\psi_N - \psi_{N-1} = 0, \tag{A6}$$

where Δ is the distance between grid points and z_1, z_N are the heights of the bottom and top boundaries, respectively. The levels $j = 0$ and $j = N + 1$ are not physical levels. Equation (A4) is used to express ψ_0, ψ_{N+1} in terms of $\psi_{1,2}$ and $\psi_{N-1,N}$, respectively; A_{N+1} and A_0 are interpolated from the two grid points below or above, respectively: $A_0 = 2A_1 - A_2$, $A_{N+1} = 2A_N - A_{N-1}$.

We may write

$$\psi_{j+1} = \alpha_j\psi_j. \tag{A7}$$

Using this with Eq. (A4), we get a recurrence relation for the α:

$$\alpha_{j-1} = \frac{A_j + A_{j-1}}{A_{j+1} + 2A_j + A_{j-1} - 2\Delta^2 B_j A_j - (A_{j+1} + A_j)\alpha_j}. \tag{A8}$$

The boundary condition at the top is used to get α_{N-1}:

$$\alpha_{N-1} = \frac{-(A_{N+1} + 2A_N + A_{N-1})}{2\Delta^2 A_N B_N - (A_{N+1} + 2A_N + A_{N-1}) - 2\Delta b(A_{N+1} + A_N)}. \tag{A9}$$

We use the above equation to start the recurrence relation to calculate $\alpha_{N-1,\ldots,1}$. This should satisfy the bottom boundary condition

$$\psi_2 = \left(1 - \Delta a - \frac{1}{2}\Delta^2 n_1^2\right)\psi_1. \tag{A10}$$

Using

$$\psi_2 = \alpha_1 \psi_1, \tag{A11}$$

we get the following equation for α_1:

$$\alpha_1 - \frac{(A_2 + 2A_1 + A_0) - 2\Delta^2 A_1 B_1 - 2a\Delta(A_2 + A_1)}{(A_2 + 2A_1 + A_0)} = 0, \tag{A12}$$

where α_1 is obtained from the recurrence relation (A8).

Equation (A12) can be satisfied only for certain values of c. We therefore have to find its zeros.

A standard MATLAB routine is used.

REFERENCES

Bretherton, F. P., 1966: Critical layer instability in baroclinic flows. *Quart. J. Roy. Meteor. Soc.*, **92,** 325–333.

Cehelsky, P., and K.-K. Tung, 1991: Nonlinear baroclinic adjustment. *J. Atmos. Sci.*, **48,** 1930–1947.

Charney, J. G., 1947: The dynamics of long waves in a baroclinic westerly current. *J. Meteor.*, **4,** 135–162.

——, and P. G. Drazin, 1961: Propagation of planetary scale disturbances from the lower into the upper atmosphere. *J. Geophys. Res.*, **66,** 83–110.

——, and M. E. Stern, 1962: On the instability of internal baroclinic jets in a rotating atmosphere. *J. Atmos. Sci.*, **19,** 159–172.

Eady, E. T., 1949: Long waves and cyclone waves. *Tellus*, **1,** 33–52.

Fullmer, J. W. A., 1982a: Calculations of the quasi-geostrophic PV gradient from climatological data. *J. Atmos. Sci.*, **39,** 1873–1877.

——, 1982b: The baroclinic instability of highly structured one-dimensional basic states. *J. Atmos. Sci.*, **39,** 2371–2378.

Green, J. S. A., 1960: A problem in baroclinic stability. *Quart. J. Roy. Meteor. Soc.*, **86,** 237–251.

Grotjahn, R., 1979: Cyclone development along weak thermal fronts. *J. Atmos. Sci.*, **36,** 2049–2074.

Gutowski, W. J., 1985: Baroclinic adjustment and mid-latitude temperature profiles. *J. Atmos. Sci.*, **42,** 1733–1745.

——, L. E. Branscome, and D. A. Stewart, 1989: Mean flow adjustment during life cycles of baroclinic waves. *J. Atmos. Sci.*, **46,** 1724–1737.

Kuo, H. L., 1979: Baroclinic instabilities of linear and jet profiles in the atmosphere. *J. Atmos. Sci.*, **36,** 2360–2378.

Lindzen, R. S., 1993: Baroclinic neutrality and the tropopause. *J. Atmos. Sci.*, **50,** 1148–1151.

——, 1994a: The effect of concentrated PV gradients on stationary waves. *J. Atmos. Sci.*, **51,** 3455–3466.

——, 1994b: The Eady problem for a basic state with zero PV gradients but $\beta \neq 0$. *J. Atmos. Sci.*, **51,** 3221–3226.

——, and B. F. Farrell, 1980a: The role of polar regions in global climate, and the parameterization of global heat transport. *Mon. Wea. Rev.*, **108,** 2064–2079.

——, and ——, 1980b: A simple approximate result for the maximum growth rate of baroclinic instabilities. *J. Atmos. Sci.*, **37,** 1648–1654.

——, ——, and K. K. Tung, 1980: The concept of wave overreflection and its application to baroclinic instability. *J. Atmos. Sci.*, **37,** 44–63.

Morgan, M. C., 1995: An observationally and dynamically determined basic state for the study of synoptic-scale waves. Ph.D. thesis, Massachusetts Institute of Technology, 123 pp. [Available from PAOC, 54-1424, Massachusetts Institute of Technology, Cambridge, MA 02139.]

Randel, W. J., and J. L. Stanford, 1985: The observed life cycle of a baroclinic instability. *J. Atmos. Sci.*, **42,** 1364–1373.

Rhines, P. B., and W. R. Young, 1982: Homogenization of potential vorticity in planetary gyres. *J. Fluid Mech.*, **122,** 347–367.

Simmons, A. J., and B. J. Hoskins, 1978: The life cycles of some nonlinear baroclinic waves. *J. Atmos. Sci.*, **35,** 414–432.

Snyder, C. M., and R. S. Lindzen, 1988: Upper-level baroclinic instability. *J. Atmos. Sci.*, **45,** 2445–2459.

Stone, P. H., 1978: Baroclinic adjustment. *J. Atmos. Sci.*, **35,** 561–570.

——, and L. Branscome, 1992: Diabatically forced nearly inviscid eddy regimes. *J. Atmos. Sci.*, **49,** 2446–2459.

——, and B. Nemet, 1996: Baroclinic adjustment: A comparison between theory, observation, and models. *J. Atmos. Sci.*, **53,** 1663–1674.

Sun, D. Z., and R. S. Lindzen, 1994: A PV view of the zonal mean distribution of temperature and wind in the extratropical troposphere. *J. Atmos. Sci.*, **51,** 757–772.

Thorncroft, C. D., B. J. Hoskins, and M. E. McIntyre, 1993: Two paradigms of baroclinic-wave life-cycle behaviour. *Quart. J. Roy. Meteor. Soc.*, **119,** 17–55.